Ocular Dominance Predicts Neither Strength Nor Class of Disparity Selectivity With Random-Dot Stimuli in Primate V1

Jenny C. A. Read and Bruce G. Cumming

Laboratory of Sensorimotor Research, National Eye Institute, National Institutes of Health, Bethesda, Maryland 20892-4435

Read, Jenny C. A. and Bruce G. Cumming. Ocular dominance predicts neither strength nor class of disparity selectivity with random-dot stimuli in primate V1. *J Neurophysiol* 91: 1271–1281, 2004. First published October 1, 2003; 10.1152/jn.00588.2003. We address two unresolved issues concerning the coding of binocular disparity in primary visual cortex. Experimental studies and theoretical models have suggested a relationship between a cell's ocular dominance, assessed with monocular stimuli, and its tuning to binocular disparity. First, the disparity energy model of disparity selectivity suggests that there should be a correlation between ocular dominance and the strength of disparity tuning. Second, several studies have reported a relationship between ocular dominance and the shape of the disparity tuning curve, with cells dominated by one eye more likely to have disparity tuning of the tuned-inhibitory type. We investigated both of these relationships in single neurons recorded from the primary visual cortex of awake fixating macaques, using dynamic random-dot patterns as a stimulus. To classify disparity tuning curves quantitatively, we develop a new measure of symmetry, which can be applied to any function. We find no evidence for any correlation between ocular dominance and the nature of disparity tuning. This places constraints on the circuitry underlying disparity tuning.

INTRODUCTION

Humans and other animals with front-facing eyes have the remarkable ability to perceive stereoscopic depth based on small disparities between the retinal images. The neural processing underlying this ability is believed to begin in primary visual cortex (V1), which contains many cells that vary their firing rate as a function of the binocular disparity present in the stimulus (Barlow et al. 1967; Nikara et al. 1968). The properties of these cells have been the subject of extensive investigation (Anzai et al. 1999a,b; Cumming and Parker 1997, 1999; Ohzawa et al. 1996, 1997, 1990; Poggio and Fischer 1977; Poggio and Talbot 1981; Poggio et al. 1985, 1988; Prince et al. 2002b).

A mathematical model, known as the disparity energy model (Ohzawa 1998; Ohzawa et al. 1990), has been developed to explain how disparity tuning can arise physiologically. A central feature of the energy model is that spatial summation is linear until after inputs from the 2 eyes are summed. An output nonlinearity after binocular combination generates disparity selectivity. In its original form, the model exploited pairs of monocular RFs that were in quadrature phase, and the output nonlinearity was squaring. Thus the model computed a form of binocular contrast energy; hence the name. If either of these properties is changed—for example, if the inputs from the 2 eyes are not equally weighted—the model no longer strictly computes energy. However, we shall continue to use the term "energy model" to describe this generalized class of models (linear binocular summation combined with an output nonlinearity), which behave in the same general way as the energy model.

Cells that are sensitive to binocular disparity are clearly receiving information from both eyes. One might thus expect a relationship between ocular dominance and the strength of disparity tuning, whereby cells that show little or no response to monocular stimulation in one eye would show poor disparity selectivity, whereas cells that are very sensitive to binocular disparity would respond equally well to monocular input in either eye. Such a relationship is predicted by the disparity energy model, but the experimental evidence is mixed. Smith et al. (1997), working in monkey V1, reported a tendency for cells with balanced ocular dominances to be the most sensitive to phase disparities in binocular grating stimuli. However, this relationship between ocular dominance and binocular interaction was weak (their Fig. 7), and its statistical significance was not assessed. Gardner and Raiten (1986), working in cat A17/18, reported a relationship in the opposite direction: strongly disparity tuned neurons tended to be very unequally driven by monocular stimulation, whereas neurons that gave similar responses to monocular inputs in either eye tended to have little or no disparity tuning. Other workers, both in monkey and in cat, found little evidence of any correlation between ocular dominance and the strength of disparity tuning (LeVay and Voigt 1988; Ohzawa and Freeman 1986b; Poggio and Fischer 1977; Prince et al. 2002b).

An alternative suggestion is that ocular dominance is correlated not so much with the strength of disparity tuning, but with the particular form it takes. Poggio and Fischer (1977) developed a widely used scheme for describing the most common types of disparity tuning. These authors recognized 4 groups: *1*) "tuned-excitatory" (TE) neurons, which increased their firing rate when the stimulus had zero disparity; *2*) "tuned-inhibitory" (TI) neurons, which decreased their firing for zero disparity; *3*) "near" cells, which increased their firing for crossed disparities and were suppressed by uncrossed disparities; and *4*) "far" cells, which increased their firing for uncrossed disparities and were suppressed by crossed disparities. In their original study, Poggio and Fischer (1977) noted that cells of the near, far, and tuned-inhibitory classes tend to respond to monocular stimulation in only one eye, while remaining silent for monocular stimulation in the other eye. (For short, we shall refer to such cells as "monocular," although

Address for reprint requests and other correspondence: J. Read, NIH, 49/2A50 Convent Dr., Bethesda, MD 20892-4435 (E-mail: jcr@lsr.nei.nih.gov).

clearly if they are disparity-tuned they must receive information from both eyes; conversely we shall refer to cells that respond roughly equally to monocular stimulation in either eye as "binocular.") This observation has been supported by several subsequent studies, both in monkey (Fischer and Poggio 1979; Gonzalez et al. 2001) and in cat (Fischer and Krueger 1979; Maske et al. 1986), although Poggio found in later experiments that the tendency for near/far/tuned-inhibitory neurons to be dominated by one eye was less striking than he had reported earlier (Poggio and Talbot 1981).

There is potentially a simple rationale for the reported correlation between ocular dominance and tuning class. Suppose tuned-excitatory neurons receive excitatory input from both eyes, whereas tuned-inhibitory neurons receive excitatory input from one eye and inhibitory input from the other (Poggio et al. 1988; Read et al. 2002). This could explain both why tuned-inhibitory neurons appear monocular and why they have a dip in their disparity tuning curve (the inhibitory eye suppresses the cell's response at a particular disparity). However, this rationale cannot be used within the framework of the energy model of disparity selectivity. This model requires there to be both excitatory and inhibitory inputs from each eye, to achieve linear binocular combination (Ohzawa and Freeman 1986b; Ohzawa et al. 1990). In the energy model, the shape of the disparity tuning curve depends only on the arrangement of receptive field subregions in the 2 eyes. If the arrangement of subregions is identical in the 2 eyes, the energy model predicts that the disparity tuning curve is tuned-excitatory, with a central peak at a preferred disparity. If an ON subregion in the left eye is paired with an OFF subregion in the right eye, the energy model predicts a tuned-inhibitory disparity tuning curve, in which firing is suppressed at a particular null disparity. There is therefore no reason to expect a correlation between ocular dominance and disparity tuning class. If the reported correlation is to be consistent with the energy model, there must be an arbitrary relationship between the ocular dominance and the relative arrangement of receptive field subregions in the 2 eyes. No such relationship is found (Ohzawa et al. 1996). Thus the reported correlation presents a challenge to the energy model.

However, before making any changes to the energy model, we need to be sure that the reported correlation between ocular dominance and disparity tuning class really holds. All the studies cited so far have been purely qualitative, so it is unclear how much weight to place on their conclusions. There have been only 2 quantitative studies addressing this issue. In cat areas 17 and 18, LeVay and Voigt (1988) broadly supported the correlation between ocular dominance and tuning class, but suggested that this reflected a relationship between ocular dominance and preferred disparity, cells with balanced inputs from the 2 eyes tending to have preferred disparities near zero. In the monkey, Prince et al. (2002b) measured disparity tuning with random-dot patterns in both simple and complex cells. They found no significant relationship between ocular dominance and class of disparity tuning. This is the only quantitative study in the monkey and the only quantitative study restricted to V1. There was some suggestion of a difference between their 2 monkeys; in one monkey there did appear to be a slight tendency for binocular neurons to be tuned-excitatory. In addition, this study used the phase of a Gabor function fitted to the disparity tuning curve to classify cells into the different

classes and did not look for a relationship between ocular dominance and preferred disparity like that reported by LeVay and Voigt (1988).

Currently, it is thus unclear precisely what if any relationship exists between ocular dominance measured monocularly and the strength or class of disparity tuning measured binocularly. Concerning the strength, the evidence is conflicting, with different studies claiming variously a positive, negative, or zero correlation between ocular dominance and the strength of disparity tuning. Concerning the class, several qualitative studies suggest that there is a relationship between ocular dominance and the class of disparity tuning, with tuned-inhibitory cells more likely to be "monocular" and tuned-excitatory "binocular." Quantitative studies have generally failed to bear this out, but in each case there have been reservations that prevent definitive conclusions. One difficulty is that the conclusions from quantitative studies may depend on how the early qualitative classification is converted into quantitative criteria.

In the course of a detailed study of the energy model predictions (Read and Cumming 2003), we gathered a large amount of data on the responses of disparity-tuned cells in monkey striate cortex to monocular and binocular random-dot stimulation. In this paper, we analyze this data set and investigate different ways of converting the original qualitative classifications into quantitative criteria, in an attempt to provide a definitive answer as to whether any aspect of disparity tuning can be predicted from a cell's monocular response strength.

METHODS

Detailed descriptions of the general procedures have appeared elsewhere (Cumming and Parker 1999; Prince et al. 2002b; Read and Cumming 2003). In brief, single-unit activity was recorded from primary visual cortex (V1) of 2 awake monkeys (*Macaca mulatta*) trained to maintain fixation while viewing stimuli for fluid reward. All protocols were approved by the Institute's Animal Care and Use Committee and complied with Public Health Service policy on the humane care and use of laboratory animals.

Stimuli were generated on a Silicon Graphics Octane workstation and presented on 2 Eizo Flexscan F980 monitors (mean luminance 41.1 cd/m^2, contrast 99%, frame rate 72 Hz) viewed by a Wheatstone stereoscope, in which the monitors are viewed through mirrors positioned in front of the animal's eyes. At the viewing distance used (89 cm) each pixel in the 1280 × 1024 display subtended 1.1 min arc, and anti-aliasing was used to render with subpixel accuracy. Glass-coated platinum–iridium electrodes (FHC) were placed transdurally each day. Electrode position was controlled with a custom-made microdrive that used an ultralight stepper motor mounted directly onto the recording chamber.

Stimulus presentation was initiated by the monkey maintaining fixation on a binocularly presented spot to within ±1°. Fixation had to be maintained at this accuracy for 2.1 s to earn a fluid reward. Four stimuli were presented during a trial, each stimulus lasting 420 ms, with successive stimuli separated by 100 ms.

Stimuli

The stimuli were dynamic random-dot stereograms, composed of black and white dots, scattered at random on a gray background. The dots were usually 5 × 5 pixels (0.1° × 0.1°) at 50% density; for some cells, a different size was used if this enhanced the response rate. The central disparate region (usually 3° in diameter) was surrounded by an annular region of dots whose disparity was always zero. The surround

region was always large enough to enclose the central target even at the largest disparities tested. A new random stereogram was generated every frame (72 Hz). Experimental disparities were applied along the axis orthogonal to each neuron's preferred orientation, assessed using grating stimuli. The initial test for disparity selectivity used stimulus disparities from -1.2 to $+1.2°$, with the range -0.6 to $+0.6°$ covered in steps of $0.1°$, and the larger disparities in steps of $0.2°$. If necessary for adequate sampling of the disparity tuning, a larger range of disparities was sometimes used, and the central region of the curve was sometimes sampled more finely. Binocularly uncorrelated random-dot patterns and monocular patterns were also presented, interleaved with the disparate patterns. Uncorrelated patterns are equivalent to infinite disparity: because receptive fields are finite in space, as disparity is increased the disparity tuning curve must eventually approach the response to uncorrelated patterns. Importantly, the spatial properties of the stimulus used to assess ocularity were identical to the spatial properties of the stimulus used to measure disparity tuning. Previous studies, especially those using random-dot patterns, have not always done this (e.g., Prince et al. 2002a).

Data transformation

The variance of neuronal firing rates is typically proportional to the mean firing rate (Dean 1981). This complicates the analysis of neuronal data: curves cannot be fit to mean firing rates without some correction for the changing variance. This complication can be avoided if we first transform neuronal firing rates by taking the square root. For all but the smallest firing rates, the variance of $\sqrt{\text{firing rate}}$ is roughly independent of the mean, greatly simplifying the analysis (Prince et al. 2002b). For this reason, we perform all statistical data analysis on $\sqrt{\text{firing rate}}$

Data analysis

DISPARITY TUNING. To quantify the strength of disparity tuning, we used the disparity discrimination index introduced by Prince et al. (2002b)

$$\text{DDI} = \frac{R_{\max} - R_{\min}}{R_{\max} - R_{\min} + 2\text{RMS}_{\text{error}}} \tag{1}$$

where $R_{\max}$ and $R_{\min}$ are the maximum and minimum values of the mean $\sqrt{\text{firing rate}}$ obtained at fixed disparity, and $\text{RMS}_{\text{error}}$ is the square root of the residual variance around the mean $\sqrt{\text{firing rate}}$ at each disparity, including the response to uncorrelated stimuli (effectively, infinite disparity). This is similar to the more straightforward binocular interaction index (BII; Ohzawa and Freeman 1986a; Smith et al. 1997)

$$\text{BII} = (R_{\max} - R_{\min})/(R_{\max} + R_{\min}) \tag{2}$$

but avoids problems associated with the BII. For example, a cell that fires less on average is more likely to have a larger BII simply by chance, so the BII is inversely correlated with mean firing rate (Prince et al. 2002b). In contrast, the DDI is larger for a cell where the modulation in mean firing as a function of disparity is relatively small, but is highly reliable, than for a noisy cell where the range ($R_{\max} - R_{\min}$) may be large but appears to be attributable to finite sampling of a noisy variable rather than genuine disparity tuning. Thus the DDI more effectively captures what we intuitively mean by disparity tuning.

To allow a cell into the study, we required that binocular random-dot stimuli at the optimal disparity elicit a response of ≥ 10 spikes/s. To proceed to quantitative analysis of the disparity tuning curve it was important that the disparity-induced changes in firing rate were reliable. We therefore required that *1*) ANOVA should indicate a significant ($P < 0.05$) main effect of disparity and *2*) the DDI should exceed 0.375.

OCULAR DOMINANCE. Monocular random-dot stimuli were presented interleaved with the binocular stimuli. We define the ocularity index (OI) as

$$\text{OI} = \frac{L - R}{L + R} \tag{3}$$

where L and R are the mean firing rates for monocular random-dot stereograms in the left and right eyes, respectively. We do not include an $\text{RMS}_{\text{error}}$ term as we did for the DDI (*Eq. 1*) because we are not interested in the question of how well monocular stimuli in the 2 eyes can be distinguished, only in their relative strength. We verified that our conclusions are not significantly different whether we define OI as in *Eq. 3*, or in terms of $\sqrt{\text{firing rate}}$, or analogously to the DDI above, including a residual variance term.

The OI varies between $+1$ (entirely dominated by left eye) and -1 (entirely dominated by right eye). The absolute value is the monocularity index (MI) (LeVay and Voigt 1988; Prince et al. 2002b)

$$\text{MI} = \frac{|L - R|}{L + R} \tag{4}$$

$\text{MI} = 1$ indicates that no response was elicited by monocular stimulation in one of the eyes (pure monocular); $\text{MI} = 0$ indicates that the same response was elicited in each eye (pure binocular).

SIGNIFICANCE. We adopted a significance criterion of $P \leq 0.05$ throughout.

Curve fitting

We fitted disparity tuning curves with Gabor functions, the product of a sinusoid carrier and a Gaussian envelope, which were established to give a good description of disparity tuning in most cells (Cumming and Parker 1997; Ohzawa et al. 1997; Prince et al. 2002b). Gabors have 6 free parameters: the spatial frequency f and phase ϕ of the carrier cosine, the SD σ, amplitude A and center δ_0 of the Gaussian envelope, and the baseline firing rate B about which the sinusoid oscillates, representing the response to binocularly uncorrelated stimuli

$$G(\delta) = B + A \exp\left(-\frac{(\delta - \delta_0)^2}{2\sigma^2}\right) \cos\left[2\pi f(d - \delta_0) + \phi\right] \tag{5}$$

Because firing rates can never be negative, we half-wave–rectified the function $G(\delta)$, replacing negative values of the fit function with zeros. To avoid problems caused by the nonconstant variance of neuronal firing rates (see above), we fitted the square root of a half-wave–rectified Gabor function to the square root of neuronal firing rates. We used Matlab's FMINSEARCH function (www. mathworks.com) to find the parameters that minimized the sum-of-square residuals between the transformed data and the sqrt-Gabor. Subsequent analyses made use of the smooth curve described by the Gabor fits, but did not directly use the parameters of the Gabor fit. Thus it was important that the fits describe the data well, but not important that the parameters of the Gabor be well constrained. For example, we found, like Prince et al. (2002b), that many curves could be adequately described by a Gaussian curve. The Gabor fit was then itself very close to Gaussian in form, and our subsequent analyses will have reflected this.

Classification of disparity tuning

In seeking to investigate these issues quantitatively, we face the problem of how to convert the subjective descriptions of the different classes into quantitative criteria. The major problem is that the initial description assumes that cells belong to discrete classes, which are specified by several properties such as symmetry, range of disparity tuning, and preferred disparity. More recent work demonstrates that

there is in fact a continuum. This raises the question of how to classify cells that fall in between the original classes, sharing properties originally associated with different classes. In recent years, the TE/TI/near/far labels have been reinterpreted in terms of the symmetry of the disparity tuning curve (DeAngelis et al. 1995; Freeman and Ohzawa 1990; Nomura et al. 1990; Ohzawa et al. 1990; Prince et al. 2002b; Read et al. 2002; Tsao et al. 2003). Figure 1 shows ideal disparity tuning curves from the different classes as defined in these more recent studies. Rather than being distinct categories, the different classes form a continuum that can be parameterized by the phase of the sinusoidal component of a Gabor function (Freeman and Ohzawa 1990; Ohzawa et al. 1996; Prince et al. 2002a). Tuned-excitatory curves have a phase of 0°, whereas tuned-inhibitory curves have a phase of 180°. Both these curves are even-symmetric; that is, they are unchanged by reflection about their center. The labels near/far are applied to odd-symmetric tuning curves [sometimes called asymmetric (Fischer and Krueger 1979; Gonzalez et al. 2001; Poggio et al. 1988; Tsao et al. 2003)], with phases of ±90°. Later, we discuss potential problems with this interpretation of the old qualitative labels.

Extracting reliable measures of symmetry

Like these previous workers, we used the symmetry of the Gabor fitted to the disparity tuning curve to classify the cells into the subtypes identified by Poggio and Fischer (1977). However, we did not simply use the phase of the fitted Gabor. This is a good measure of symmetry for relatively narrow-band Gabors, but can give misleading results for broad-band Gabors. Functions very close to even-symmetric can be produced by a Gabor with a phase close to 90°, if the spatial period of the carrier sinusoid is much larger than the SD of the Gaussian envelope. Under these circumstances, the Gabor is close to a Gaussian. The sinusoidal carrier contributes little to the fit, so its spatial frequency and phase are very poorly constrained. Figure 2 shows this for one example cell, duf091. Figure 2A shows the experimental disparity tuning curve and the Gabor fit. Clearly, this would be classified by eye as tuned-excitatory. However, the phase of the fitted Gabor is −69°, which is closer to −90° ("far") than to 0°. Figure 2B shows how this has happened. The heavy line is the Gabor fit (with a different vertical scale than that in Fig. 2A). The dashed line shows the Gaussian envelope of the Gabor and the dotted line its sinusoidal carrier; thus the heavy curve is the product of the other 2 curves relative to the baseline. The carrier is close to odd-symmetric about the center of the Gaussian (vertical line). Because the spatial period of the carrier is so long, however, this odd symmetry is not apparent, and the resultant fit is nearly even-symmetric. Thus the Gabor phase does not capture the symmetry of the fitted Gabor function. Note however that the Gabor fit nonetheless provides a good description of the data.
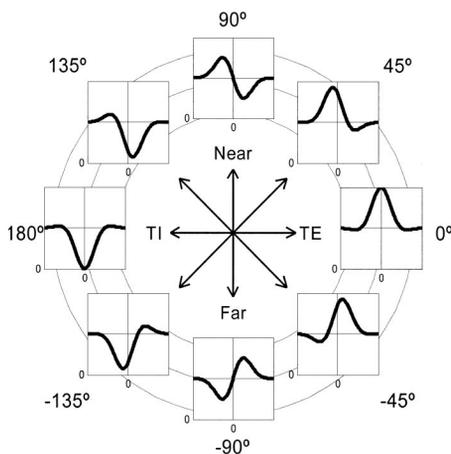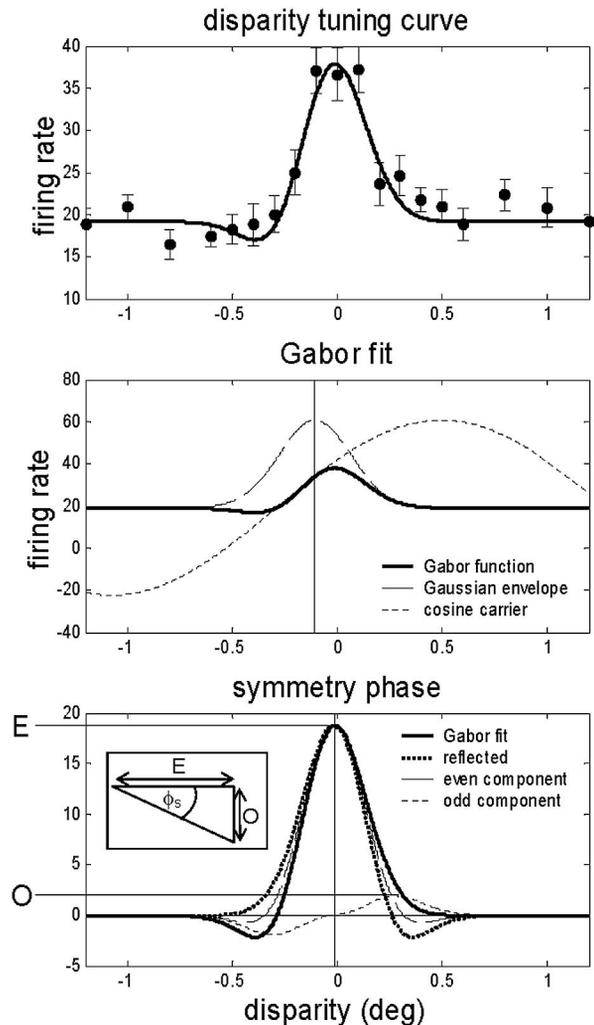

FIG. 2. Calculation of symmetry phase for an example Gabor function. *A*: experimental disparity tuning curve (black dots; error-bars are SE) and fitted Gabor function (black curve) for duf091. The phase of the fitted Gabor is −69°, which would be classified as "far". *B*: Gabor fit divided into its components: a Gaussian envelope (dashed line) and a cosine carrier (dotted line). Period of the carrier is much wider than the SD of the Gaussian. *C*: Gabor fit resolved into its even and odd components (thin lines, see legend): the Gabor function (solid line) is the sum of these. Horizontal lines labeled E and O show the peaks of the even and odd components. These are used to calculate the symmetry phase ϕ_s as shown in the *inset*: in this example *O* is negative (peak to the right of the centroid), and consequently so is ϕ_s. Dotted line is the fitted function reflected about the centroid, which is used in the calculation of the odd and even components. Mean of the function and its reflection provides the even component. Half the difference between the function and its reflection gives the odd component.

Therefore rather than relying on the parameters of the Gabor fit, we measured the symmetry of the fitted curve itself, using a measure we term the *symmetry phase* ϕ_s. This process is shown in Fig. 2*C*. We calculate the centroid of the fitted function, defined as

$$\bar{d} = \frac{\int_{+\infty}^{-\infty} d\delta |D(\delta)|\delta}{\int_{-\infty}^{+\infty} d\delta |D(\delta)|} \tag{6}$$

where $D(\delta)$ is the disparity-modulated component of the fitted function (i.e., the fit minus its baseline B). This is indicated by the vertical line in Fig. 2*C*. Note that whereas the center of the Gaussian envelope

FIG. 1. Idealized members of the 4 classes of disparity tuning: tuned-excitatory (0°), near (90°), tuned-inhibitory (180°), and far (−90°).

is offset from the peak of the tuning curve (vertical line in Fig. 2*B*), the centroid is close to the peak. To express the disparity-modulated component as a sum of an even and an odd component, we reflect the disparity-modulated component about the centroid (dotted line in Fig. 2*C*); we denote this $D'(\delta)$. The even component of the disparity-modulated function $D(\delta)$ about the centroid is the mean of the disparity-modulated function and its reflection, $D_{\text{even}}(\delta) = [D(\delta) + D'(\delta)]/2$, whereas the odd component is half their difference $D_{\text{odd}}(\delta) = [D(\delta) - D'(\delta)]/2$. These are shown in Fig. 2*C*; the Gabor fit is the sum of these (and the baseline). The peaks of the two components are indicated ("E" and "O"). The even component is much larger than the odd component, reflecting the nearly even symmetry of the fitted curve. To quantify this, we first summarize each component into a single number, respectively, E and O. In each case, the magnitude of the number is the component's maximum departure from zero. The sign of E describes whether the maximum departure of the even component is above $(+)$ or below $(-)$ the horizontal axis. The sign of O describes whether the peak of the odd component occurs to the left $(+)$ or right $(-)$ of the centroid. We then define the *symmetry phase angle* based on the ratio of E and O, as

shown in the *inset* in Fig. 2*C* $[\phi_s = \arctan(O/E)]$. This means that curves dominated by their even component have symmetry phases close to 0 or 180°; curves dominated by their odd component have symmetry phases close to $\pm 90°$. The signs given to E and O mean that the symmetry phase angle has a range of 360°. We classify cells with symmetry phases within $\pm 60°$ of zero to be tuned-excitatory-type, those within $\pm 60°$ of 180° to be tuned-inhibitory-type, those within $\pm 30°$ of $-90°$ to be far-type, and those within $\pm 30°$ of 90° to be near-type. For the cell shown in Fig. 2, the symmetry phase is $-6°$, meaning the cell is classified as tuned-excitatory.

Figure 3 explores how the symmetry phase is related to the Gabor phase and to the shape of the disparity tuning curve. The *main panel* shows the symmetry phase plotted against the phase of the fitted Gabor function, for the 118 disparity-selective neurons whose tuning functions were well described by a Gabor. The solid line shows the identity. For most cells, the 2 measures are in good agreement. This is especially clear at $\phi = 0$ and 180°: that is, cells that are classified as even-symmetric (TE/TI) on the basis of their Gabor phase will be classified in the same way by their symmetry phase. However, at intermediate phases, especially close to $\phi = \pm 90°$, discrepancies

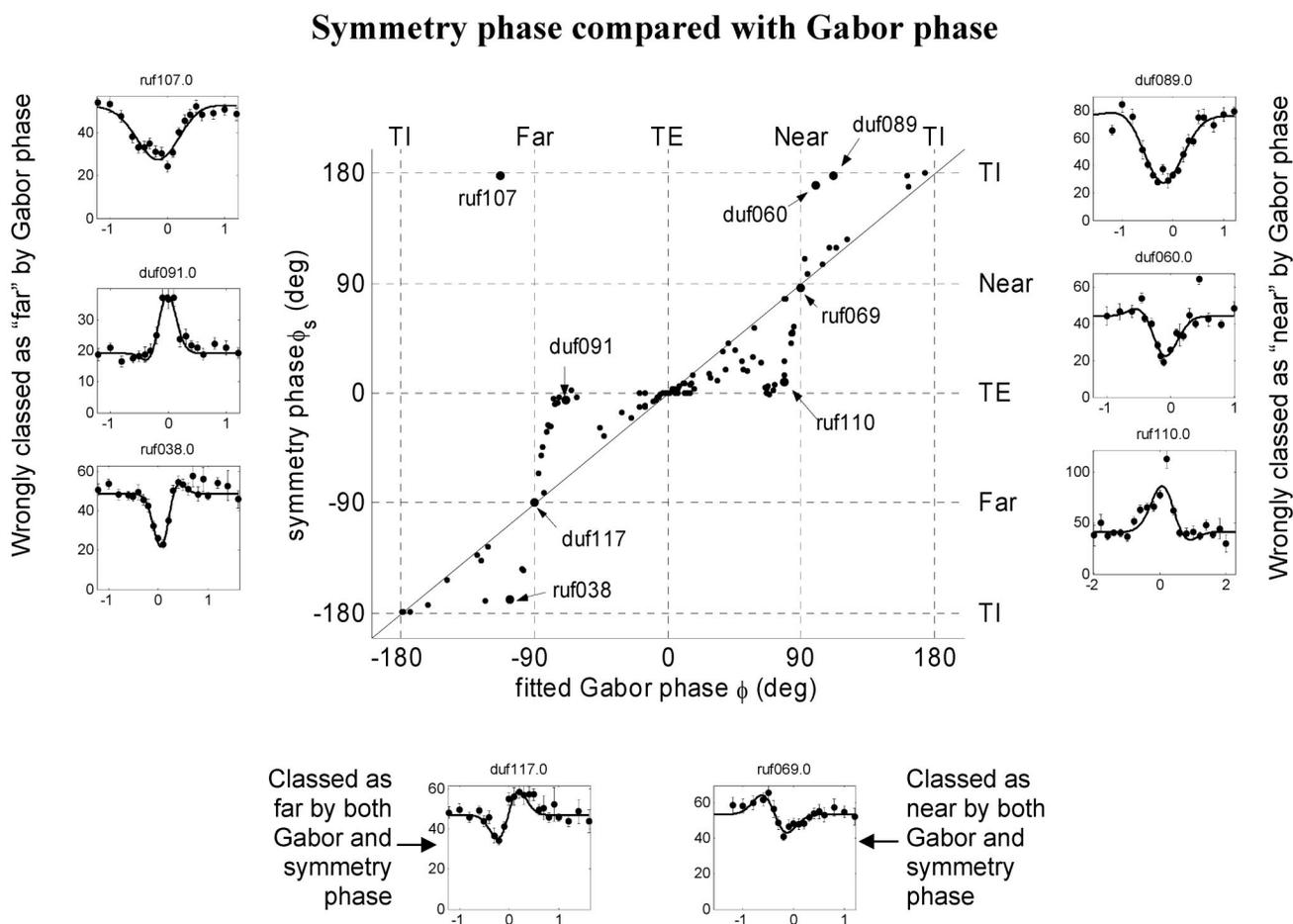## Symmetry phase compared with Gabor phase

FIG. 3. *Main panel*: scatterplot of the symmetry phase plotted against the Gabor phase for 118 disparity-selective cells whose tuning was well described by a Gabor function. Phases have been defined to lie within the range $\pm 180°$. Solid line shows the identity. Dotted lines mark the phases for the different classes of disparity tuning: tuned-excitatory (TE): phase 0°, tuned-inhibitory (TI): phase $\pm 180°$; near, phase 90°; far, phase $-90°$. Note that the top and bottom edges of the plot represent the same values, as do the left and right edges. Around the edges are *inset disparity tuning curves* for the 8 cells labeled in the main plot; these are indicated with larger symbols in the main panel. *Left*: 3 cells that would be incorrectly classified as "far" on the basis of their Gabor phase ϕ, but are correctly classified as even-symmetric by the symmetry phase ϕ_s. ruf107: $\phi = -113°$ (near), $\phi_s = 178°$ (TI). duf091: $\phi = -69°$ (near), $\phi_s = -6°$ (TE). ruf038: $\phi = -106°$ (near), $\phi_s = -169°$ (TI). *Right*: 3 cells that would be incorrectly classified as "near" on the basis of their Gabor phase ϕ, but are correctly classified as even-symmetric by the symmetry phase ϕ_s. duf089: $\phi = 112°$ (far), $\phi_s = 178°$ (TI). duf060: $\phi = 100°$ (far), $\phi_s = 170°$ (TI). ruf110: $\phi = 79°$ (far), $\phi_s = 9°$ (TE). *Bottom*: 2 cells that are correctly classified as far/near by both Gabor and symmetry phase. duf117: $\phi = \phi_s = -90°$ (far); ruf069: $\phi = 90°$, $\phi_s = 86°$ (near).

occur. Several cells that would be classified as odd-symmetric (near/far) on the basis of their Gabor phase are classified as even-symmetric (TE/TI) by the symmetry index. Six examples of such cells are shown to the *left* and *right* of the *main panel* in Fig. 3*A*. On the *left* we have 3 examples (ruf107, duf091, and ruf038) that are all close to −90° on the horizontal axis and were thus classified as "near" on the basis of their Gabor phase. However, inspecting their tuning curves, it seems clear that they are in fact, respectively, tuned-inhibitory, tuned-excitatory, and tuned-inhibitory. The symmetry phase classifies these cells correctly, as is apparent by comparing their position on the vertical axis. On the *right* we have 3 examples that would be classified as "far" by their Gabor phase, but that are in fact tuned-inhibitory (duf089, duf060) and tuned-excitatory (ruf110). Again, these are classified correctly with the symmetry phase. The 2 plots at the *bottom* show 2 cells (duf117, ruf069) that genuinely are odd-symmetric: these are classified correctly by both methods.

Thus the symmetry phase is similar to the Gabor phase, but more reliable because it correctly reports the symmetry even when the carrier frequency is low. It also has the advantage that it can be used with any fit function, not just Gabors.

RESULTS

Strength of disparity tuning

Monocular and binocular responses to random-dot patterns were recorded in 210 neurons, of which 180 produced a maximum firing rate of ≥10 spikes/s. Figure 4 shows the disparity discrimination index (DDI, *Eq. 1*) for these 180 cells plotted against the monocularity index (MI). The symbols distinguish cells from the 2 monkeys. On the left-hand side are cells where the inputs from the 2 eyes, assessed from the response to monocular stimulation, seem to be balanced; on the right-hand side are cells where one eye appears to dominate. Cells toward the top of the plot are those with strong disparity tuning. There is little evidence for any relationship between the 2 quantities. Although the DDI is slightly higher for the more binocular neurons than for the more monocular (DDI for the 31 cells with MI < 0.25 is 0.616 ± 0.107, mean ± SD; for the 40 cells with MI > 0.75 it is 0.568 ± 0.105), as predicted by the energy model and reported by Smith et al. (1997), this is not signifi-
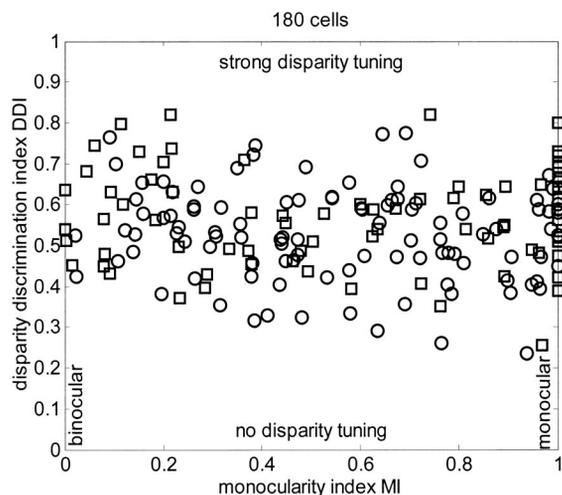

FIG. 5.   Scatterplot of the monocularity index of 118 disparity-tuned cells, plotted against the symmetry phase ϕ_s of their fitted tuning curve. This enables the cells to be classified according to their tuning type: tuned-excitatory (TE), $|\phi_s| < 60°$; tuned-inhibitory (TI), $|\phi_s| > 120°$; near/far (N/F), $60° < |\phi_s| < 120°$. Symbols as in Fig. 4. All the cells in this plot have a DDI of ≥0.375. Symbols indicate monkey (circle = Duf, square = Ruf).

cant (*t*-test, $P = 0.07$). The correlation coefficient between DDI and MI is also not significant ($r = -0.07$, $P = 0.47$). This figure includes 39 neurons that showed no disparity selectivity ($P > 0.05$, one-way ANOVA) and 3 that showed very weak selectivity ($P < 0.05$, but DDI < 0.375). Note that the DDI in such neurons is still >0 simply because of random fluctuations in firing rate.

Class of disparity tuning

Out of the 180 neurons 138 were disparity-selective, and in 118 of these 138, the disparity tuning curve was well described by a Gabor (fit explained more than 60% of variance). In the 20/138 cells for which the Gabor fit explained <60% of the variance, this failure was because the disparity tuning in these cells was noisy and unreliable. Importantly, there was no tendency for these 20 cells to show any particular type of disparity tuning. In principle, a classic "near" cell that responded to a broad range of disparities with the same firing rate (Poggio and Fischer 1977) might be difficult to fit with a Gabor. Exclusion of such responses would be misleading. In practice, however, we saw no examples of such responses, in agreement with other studies using random-dot stereograms (Prince et al. 2002b). For the 118 cells where the fit succeeded, we used the symmetry phase (ϕ_s) derived from the fitted function to classify cells into the subtypes identified by Poggio and Fischer (1977), as described in the METHODS. Restricting $|\phi_s|$ to the range 0 to 180°, cells with $|\phi_s| < 60°$ were classified as tuned-excitatory, $|\phi_s| > 120°$ as tuned-inhibitory, and the rest as odd-symmetric (near/far). On this basis, the 118 cells were classified into 86 tuned-excitatory cells, 21 tuned-inhibitory, and 11 near/far. Examples of each class are shown in Fig. 3.

Figure 5 shows MI plotted against symmetry phase. There was no significant correlation ($r = 0.12$, $P = 0.19$). The dotted lines in Fig. 5 show how the data were divided into 3 classes of disparity tuning. The mean MI of the 3 classes was 0.526 ± 0.322, 0.600 ± 0.346, and 0.577 ± 0.353, respectively (mean ± SD). None of these differed significantly from 0.5 (*t*-test), nor did the MI of one

FIG. 4.   Scatterplot of disparity discrimination index (DDI) against monocularity index (MI) for 180 cells recorded in V1. Correlation coefficient was 0.13, and the slope of a regression line was not significantly different from zero. In this and subsequent population plots, the symbols indicate the monkey in which the cell was recorded (circle = Duf, square = Ruf).
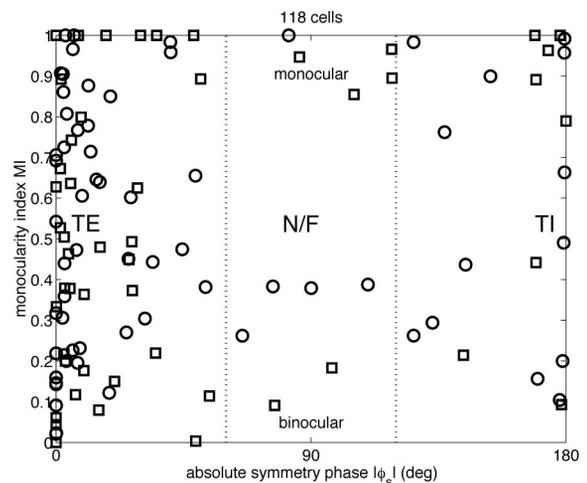
class differ significantly from that of any other (2-sample *t*-test). There appears to be an absence of near/far cells with MIs between 0.5 and 0.8 or so; however, the 3 classes showed no significant differences in variance, indicating that this gap is no larger than would be expected by random fluctuation in such a small sample [*F*-test; for TE compared with N/F, variance ratio = 0.78, degrees of freedom (*df*) = (86,11), NS; for TE compared with TI, variance ratio = 0.76, *df* = (86,21), NS]. Figure 6 shows examples of monocular and binocular cells from each tuning class. Thus we find no evidence for the relationship between ocular dominance and the class of disparity tuning reported by some previous investigators (Fischer and Krueger 1979; Fischer and Poggio 1979; Gonzalez et al. 2001; Maske et al. 1986; Poggio and Fischer 1977).

Strength and class of disparity tuning

We now ask whether strength of disparity tuning is related to class of disparity tuning. Figure 7 shows disparity discrimination index plotted against symmetry phase for the 118 cells
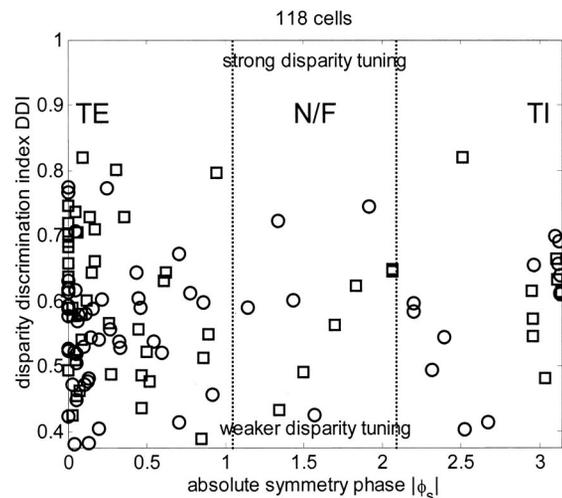

FIG. 7. Scatterplot of the disparity discrimination index (DDI) of 118 disparity-tuned cells, plotted against the absolute value of the symmetry phase. Symbols indicate monkey (circle = Duf, square = Ruf).
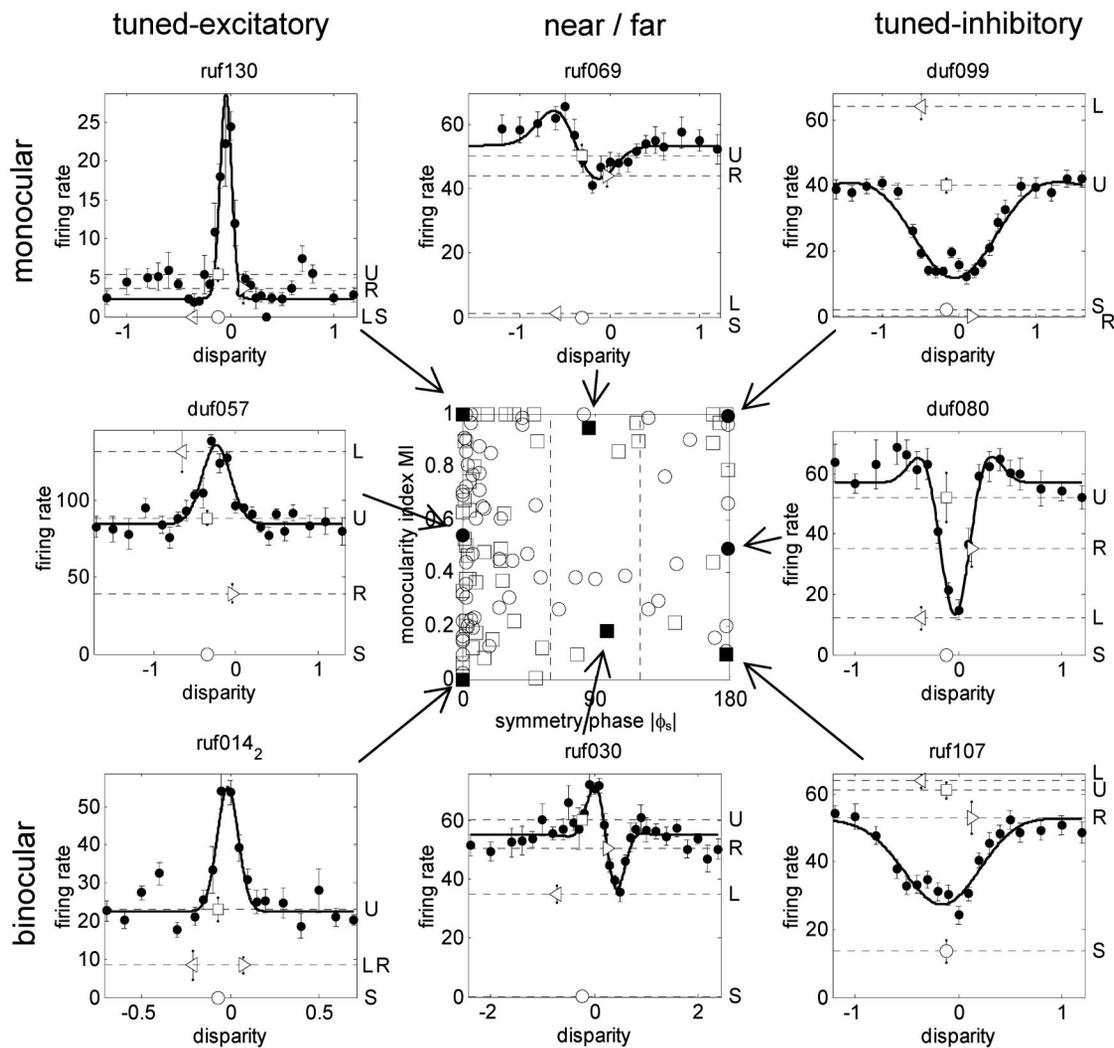

FIG. 6. Examples of monocular and binocular cells from different disparity-tuning classes. *Center panel* reproduces Fig. 5 (MI against symmetry phase). Eight example cells shown in the surround are indicated by the filled symbols. In the 8 example cells, the black dots show the mean response as a function of disparity; error-bars show SE. The solid curve is the fitted Gabor. Dotted lines show the responses to binocularly uncorrelated random dots (U□), to monocular random dots in left and right eyes (L◁, R▷), and to a blank screen of the same mean luminance (the spontaneous firing rate, S○).

whose disparity tuning was well described by a Gabor. Once again, there is no correlation ($r = 0.07$, $P = 0.45$). The mean DDI of the 86 TE cells is 0.580 ± 0.106, of the 21 TI cells is 0.597 ± 0.096, and of the 11 near/far cells is 0.589 ± 0.106; there is no significant difference between these (2-sample t-test).

In a qualitative study, Gonzalez et al. (2001) reported that there was a relationship between ocularity and strength of disparity tuning, but only for cells of the tuned-inhibitory class. To investigate this possibility quantitatively, we returned to the relationship between disparity discrimination index and monocularity (Fig. 4) and investigated it for each of the 3 disparity tuning classes separately. In no case is there a significant correlation (not shown). Thus we find no evidence in support of this suggestion.

Other ways of classifying disparity tuning

A potential reason for our failure to find a relationship between ocular dominance and class of disparity is that we may not be classifying cells in the same way as previous workers, and thus may be combining cells from several of their classes. One problem with attempts to follow earlier classification schemes is that the description of the classic near/far type observed with bar stimuli does not straightforwardly apply to random-dot stimuli. As originally described (Poggio and Fischer 1977), these had 3 identifying characteristics: *1*) their tuning curves are odd-symmetric, showing both excitation and suppression; *2*) the transition from excitation to suppression occurs at zero; and *3*) their tuning curves are broad, showing a plateau of excitation over a wide range of disparities. However, the classic plateau-type profiles appear to be obtained only with bar stimuli; in common with other studies employing random-dot patterns, we do not find such cells [see Prince et al. (2002a) and Cumming and DeAngelis (2001) for a discussion].

It may be for this reason that, in Poggio's later studies using random-dot patterns, a new class of disparity tuning is introduced (Poggio et al. 1988): tuned-near and tuned-far, describing cells whose disparity tuning curves have a single narrow peak of excitation at (respectively) a near or far disparity. The term *tuned-zero* is then used to describe cells that have a single narrow peak at zero disparity; previously, these were called tuned-excitatory. This raises a second problem. In our classification based on symmetry, such cells might all be classed together as tuned-excitatory, regardless of the disparity at which the peak occurred. This could potentially obscure a correlation between ocular dominance and disparity tuning class, if the tuned-near and tuned-far types differed from the tuned-zero class in ocularity (although no such claim has been made). In practice, it is not clear that our symmetry classification would actually confound these 3 classes of Poggio's, because even though tuned-near/far cells are initially described as if they differ from the tuned-zero cells only in the position of their peak, it subsequently becomes clear that they also differ in their symmetry: tuned-near/far cells are said to have an inhibitory region on the zero-disparity side of their peak response. This is one of the reasons why subsequent studies have concentrated on symmetry as a way of quantitatively defining the classes introduced by Poggio and coresearchers.

However, it is true that a cell with an even-symmetric peak of excitation at a near disparity would be classified as tuned-

excitatory by the symmetry criterion, and might be classified as tuned-near by eye. Thus it is clearly worth considering the possibility that our null result is due to the grouping together of tuned-zero/tuned-near/tuned-far cells. For this reason, we also considered classifying cells based on their preferred disparity. In this scheme, the classes of near/tuned-near and far/tuned-far are grouped together, which may help to uncover the correlation reported by previous studies. For example, in cat areas 17 and 18, for cells near the vertical meridian, LeVay and Voigt (1988) found a significant correlation between the ocular dominance and the preferred disparity. Cells dominated by the contralateral eye tended to prefer far disparities, cells dominated by the ipsilateral eye tended to prefer near disparities, whereas cells with balanced inputs from the 2 eyes tended to respond best to disparities near zero. In this study, we therefore also looked for a correlation between the preferred disparity and the ocularity index. [Because all the cells in our study were recorded in the left hemisphere, the ocularity index of *Eq. 3* measures whether the cell is dominated by the ipsilateral (left) or contralateral (right) eye.] We defined *preferred disparity* to be the disparity at which the maximum mean response was elicited. This is not meaningful for tuned-inhibitory cells, which were therefore omitted from this analysis (TI cells were defined, as previously, to be cells with symmetry phases within $60°$ of $\pm 180°$). No correlation between ocularity index and preferred disparity was observed. We also studied the relationship between ocularity and the centroid of the fitted Gabor. Within the energy model, this corresponds to position disparity, whereas the symmetry phase about this centroid corresponds to phase disparity. Again, there was no correlation (Fig. 8).

Ferster (1981) classified cells based on the sharpness of the peak in their disparity tuning. Although quantitative details of this classification are not provided, from the examples given in Ferster's paper, tuned-excitatory cells seem to be those whose
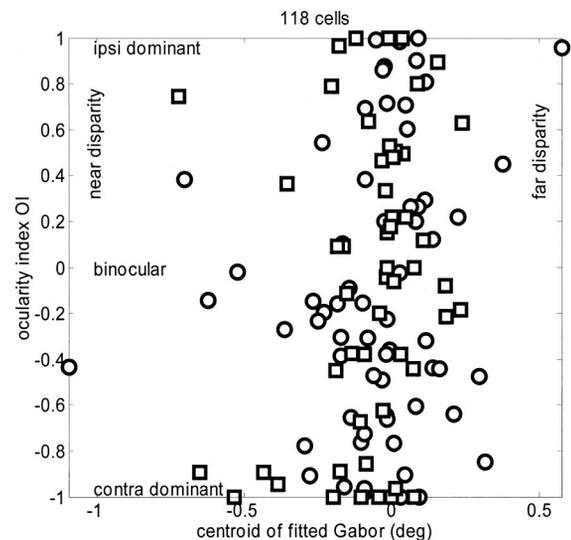

FIG. 8. Scatterplot of the ocularity index of 118 disparity-tuned cells, plotted against the centroid disparity of their fitted tuning curve (*Eq. 6*). Within the energy model, this would measure position disparity, i.e., the offset between the left and right eye receptive fields. Symbols indicate monkey (circle = Duf, square = Ruf). Correlation coefficient is 0.178, $P = 0.053$. Note that this is in the opposite direction to the correlation reported by LeVay and Voigt (1988). The near-significance is attributed to 2 outliers; if the two largest centroids are removed, P increases to 0.14.

tuning curves have several peaks and troughs, whereas the near/far cells usually have only a single trough. We therefore investigated the relationship between ocular dominance and several measures related to the spectral bandwidth of the fitted Gabor in our data, but could not uncover any correlation.

DISCUSSION

In this paper, we have carefully investigated whether, with random-dot patterns, a cell's response to monocular stimuli provides information about its sensitivity to disparity or the class of its disparity tuning curve. We found no evidence that the strength of the responses to monocular stimuli predict any aspect of the disparity tuning. Several previous workers (Le-Vay and Voigt 1988; Ohzawa and Freeman 1986b; Poggio and Fischer 1977; Prince et al. 2002b) also reported that ocular dominance is not correlated with sensitivity to disparity [although see Smith et al. (1997) and Gardner and Raiten (1986)]. However, several workers reported a correlation between ocular dominance and class of disparity tuning: "monocular" cells, which respond unequally to stimulation in the 2 eyes, are said to be found more often in the tuned-inhibitory and near/far classes (Fischer and Krueger 1979; Fischer and Poggio 1979; Gonzalez et al. 2001; LeVay and Voigt 1988; Poggio and Fischer 1977). We do not find any support for this suggestion. Although it is always impossible to prove a negative, and significant correlations might emerge if more data were collected, this seems unlikely given that our sample sizes are large compared with those in most previous studies. It is perhaps significant that the studies that reported a correlation between ocular dominance and disparity tuning class tend to be more qualitative: cells have been classified by eye and the statistical significance of the correlation has not been evaluated. Recent, more quantitative studies using objective classification criteria have failed to reveal the correlation. Although it remains possible that our objective criteria have failed to capture the features that were used subjectively by previous researchers to group cells into classes, we have investigated several different ways of implementing quantitative criteria, and so this seems unlikely. The experimental stimulus may also play a role. It may be significant that Poggio and Talbot (1981), using random-dot stimulation, reported a weaker correlation than observed previously with bars (Poggio and Fischer 1977); certainly most of the reports finding a correlation between disparity tuning class and ocularity were with bars (Fischer and Krueger 1979; Fischer and Poggio 1979; Maske et al. 1986; Poggio and Fischer 1977), whereas the only study definitively rejecting it was with random-dot patterns (Prince et al. 2002b). However, the correlation was also reported in one study using random-dot patterns (Gonzalez et al. 2001). If a correlation between ocularity and disparity-tuning shape is observed only with bar stimuli, it suggests that the relationship may reflect an artifact of changes in the monocular stimulus that accompany disparity applied to bar stimuli.

To classify disparity tuning curves as tuned-excitatory, tuned-inhibitory, near and far, we have introduced the symmetry phase ϕ_s. This is similar to the Gabor phase used by previous authors (DeAngelis et al. 1991; Nieder and Wagner 2000; Ohzawa et al. 1997; Prince et al. 2002a; Tsao et al. 2003), but is designed to capture more reliably the symmetry of the tuning curve. For narrow-band Gabors, the Gabor phase

specifies the symmetry ($\phi = 0°$, $180°$ implies even; $\phi = 90°$, $270°$ odd), but this relationship breaks down when the spatial period becomes long compared with the Gaussian envelope. Prince et al. (2002a) avoided this problem by constraining the frequency of the fitted Gabor to equal the "disparity frequency" (the peak of the Fourier amplitude spectrum of the disparity tuning curve minus its DC component). Here, we chose to allow the frequency to vary as a free parameter, to optimize the goodness of fit, and developed the symmetry phase as a way of classifying tuning curves. This gives very similar phases to those obtained with the method of Prince et al. (2002a), but has the additional advantage of being independent of the particular fit function; it could equally well be applied to extract a symmetry measure for disparity tuning curves fitted with difference-of-Gaussians or splines. To apply this method, it is of course essential that the fit be a good description of the data. We had to exclude a small number of neurons where the fit was poor (20/138). Because inspection of these data did not reveal any systematic pattern, it is unlikely that this introduced any significant bias.

The lack of any correlation between monocular properties and disparity tuning is rather striking, given that disparity tuning is presumably sculpted from the monocular inputs to the cell. It places constraints on the circuitry that underlies disparity tuning. The most widely used mathematical model of this circuitry is the disparity energy model (Ohzawa 1998; Ohzawa et al. 1990). This model is based on binocular subunits that receive inputs from left and right eyes, which are summed linearly, and output the square of the half-wave–rectified value of the sum. Although providing a generally good qualitative account of the properties of disparity-tuned cells, a number of quantitative discrepancies with experimental data are known to exist (Ohzawa et al. 1997; Prince et al. 2002b; Read and Cumming 2003; Read et al. 2002). As noted in the INTRODUCTION, the energy model does not predict the previously reported correlation between ocular dominance and class of disparity tuning, and the existence of such a correlation would be problematic for the energy model. We find no evidence for this correlation, suggesting that here at least there is no conflict between the energy model and experimental data.

However, we also noted that the energy model, at least in its original form, predicts a correlation between ocular dominance and the strength of disparity tuning. The fact that this correlation is not observed represents a challenge to the energy model. In particular, the energy model cannot explain the observation of cells whose monocular responses are severely unbalanced yet that show strong disparity tuning. This is because the energy model assumes that binocular combination is linear. This means that a binocular subunit must receive bipolar inputs from both eyes (Ohzawa et al. 1997), so each eye can have either an excitatory or an inhibitory effect, depending on the stimulus. Averaged over many monocular random-dot patterns, the inhibitory stimuli will produce no response, whereas the excitatory stimuli will elicit spikes, so the average response will always be above zero: both eyes will be able to excite the cell. Thus one would expect a correlation between ocular dominance and disparity sensitivity: all strongly disparity-tuned cells would be binocular, whereas all "monocular" cells would show weak disparity tuning. The observation of "monocular" disparity-tuned cells rules out the energy model in its
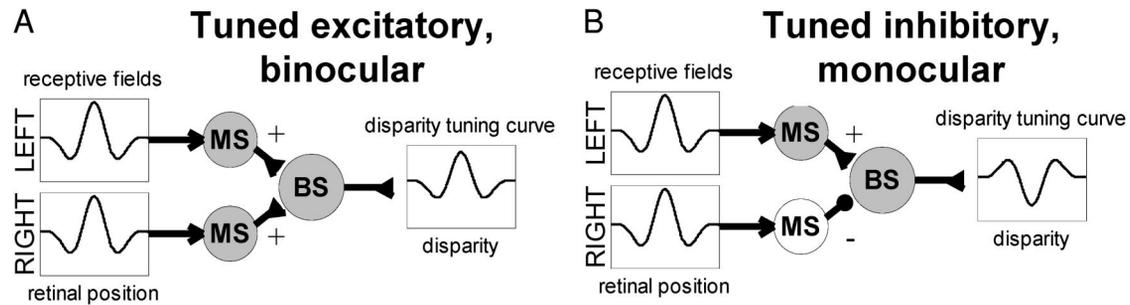
FIG. 9. Sketch of binocular cell ("BS") receiving input from left and right receptive fields. Inputs from the 2 eyes are half-wave rectified at monocular subunits ("MS") before binocular combination. Input from each eye makes either an excitatory (◀) or inhibitory (●) synapse onto the binocular subunit. *A*: both eyes make excitatory synapses; the cell is thus "binocular" in the sense that it responds to stimulation in either eye. *B*: one eye makes an inhibitory synapse and is therefore silent (MS unit for this cell is shown empty rather than shaded to signify this); the cell is thus "monocular" in that it responds to monocular stimulation in only one eye, although when tested with binocular stimuli it is disparity-tuned. Because the receptive fields in this example are identical, the disparity tuning is tuned-excitatory for the binocular cell in *A*, and tuned-inhibitory for the "monocular" cell in *B*.

simplest form. The model has to be modified to incorporate such cells.

One suggestion (Freeman and Ohzawa 1990; LeVay and Voigt 1988) is that inputs from the 2 eyes differ in their strengths, and an output threshold acts to silence the effect of input from the weaker eye. Although this could produce "monocular" cells with disparity tuning, it is unclear whether it could remove all correlation between monocularity and strength of disparity selectivity. Another possibility is that, in "monocular" disparity-tuned cells, one eye is having a purely inhibitory effect (Ferster 1981; Ohzawa and Freeman 1986a). This requires modifying the energy model to incorporate a threshold and an inhibitory synapse before binocular combination (Read and Cumming 2003; Read et al. 2002). Figure 9 sketches this circuitry. In Fig. 9*A*, both monocular cells send excitatory input to the binocular cell (◀+ denotes an excitatory synapse), so the cell is "binocular" in the sense that it responds to monocular stimulus in either eye. In contrast, in Fig. 9*B*, one eye sends excitatory and the other inhibitory input (●−). This cell would therefore be classified as "monocular," and yet it too shows disparity tuning. The existence of cells like those shown in Fig. 9*B* could explain the lack of correlation between ocular dominance and strength of disparity tuning.

However, the lack of correlation between ocular dominance and *class* of disparity tuning, although consistent with the energy model, places additional constraints on this modified version. In Fig. 9, tuned-excitatory tuning curves arise when both eyes send excitatory input to a disparity-selective cell (Fig. 9*A*), and tuned-inhibitory curves when one eye sends excitatory input and the other suppressive input (Fig. 9*B*) (Poggio et al. 1988; Read et al. 2002). This would mean that

tuned-excitatory cells would be predominantly binocular (in the sense of responding to monocular stimulation in either eye) and tuned-inhibitory cells would be predominantly "monocular." Thus this scheme would predict a correlation between ocularity and tuning type, which we do not observe.

One possible resolution is sketched in Fig. 10. This shows that, if the underlying receptive fields are 180° out of phase, a "monocular" binocular subunit has tuned-excitatory disparity tuning (Fig. 10*A*), and a "binocular" subunit has tuned-inhibitory tuning (Fig. 10*B*). Thus one explanation for the lack of correlation between ocularity and tuning type is that there is no strong preference for zero phase disparity in the underlying receptive fields. At first sight this may seem to contradict Fig. 7, which showed a strong bias toward zero symmetry phase, given that in the traditional energy model, zero symmetry phase would imply zero phase disparity. However, once we allow for cells in which one eye sends purely inhibitory input—to account for "monocular" disparity-tuned cells—then zero symmetry phase could correspond to *either* zero phase disparity *or* 180° phase disparity in the underlying receptive fields plus an inhibitory synapse. An inhibitory synapse has a similar effect to a phase inversion, so that, for example, the cell of Fig. 10*A* would have been classified as having a phase disparity of 0° in a receptive field mapping study like that of Anzai (1999a). In this scheme, tuned-excitatory cells could either have underlying receptive fields with zero phase disparity, in which case they would be "binocular," or they could have underlying receptive fields with 180° phase disparity (followed by an inhibitory synapse), in which case they would appear "monocular." This could explain why tuned-excitatory cells are observed to be as often monocular as binocular.
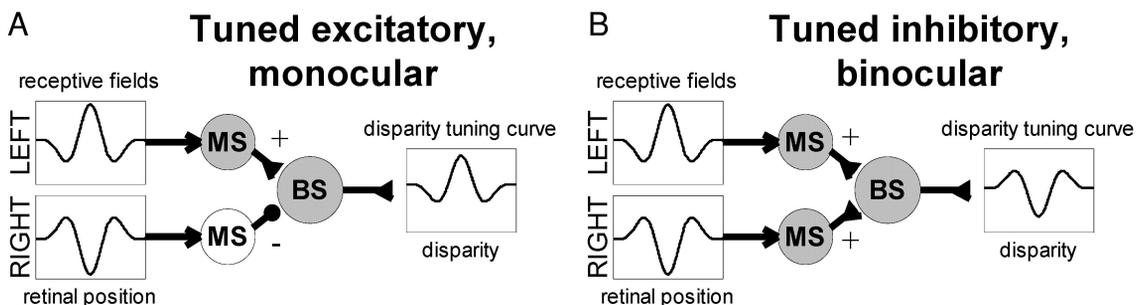

FIG. 10. Like Fig. 9, except that the receptive fields are 180° out of phase, so that now, when both eyes send excitatory input (*B*), the disparity tuning is tuned-inhibitory, and the "monocular" cell (*A*) is tuned-excitatory.

This discussion demonstrates the utility of a "null" result such as the absence of a correlation between disparity tuning class and ocular dominance. Although the results presented in this paper do not allow us to deduce the circuitry underlying disparity selectivity, they provide important constraints on the possible forms it could take.

In conclusion, we have examined a long-standing uncertainty in the literature: whether a cell's responses to monocular stimulation predict either the strength or the class of the disparity tuning. We have introduced a new quantitative way of classifying disparity tuning curves into symmetry groups, which can be used with any fitted function. We found no evidence that monocular responses to random-dot patterns carry any information about disparity tuning. This immediately rules out a number of simple suggestions for how monocular inputs may be combined to yield disparity tuning.

REFERENCES

Anzai A, Ohzawa I, and Freeman RD. Neural mechanisms for processing binocular information. I. Simple cells. *J Neurophysiol* 82: 891–908, 1999a.

Anzai A, Ohzawa I, and Freeman RD. Neural mechanisms for processing binocular information. II. Complex cells. *J Neurophysiol* 82: 909–924, 1999b.

Barlow HB, Blakemore C, and Pettigrew JD. The neural mechanisms of binocular depth discrimination. *J Physiol* 193: 327–342, 1967.

Cumming BG and DeAngelis GC. The physiology of stereopsis. *Annu Rev Neurosci* 24: 203–238, 2001.

Cumming BG and Parker AJ. Responses of primary visual cortical neurons to binocular disparity without depth perception. *Nature* 389: 280–283, 1997.

Cumming BG and Parker AJ. Binocular neurons in V1 of awake monkeys are selective for absolute, not relative, disparity. *J Neurosci* 19: 5602–5618, 1999.

Dean AF. The variability of discharge of simple cells in the cat striate cortex. *Exp Brain Res* 44: 437–440, 1981.

DeAngelis GC, Ohzawa I, and Freeman R. Depth is encoded in the visual cortex by a specialised receptive field structure. *Nature* 352: 156–159, 1991.

DeAngelis GC, Ohzawa I, and Freeman RD. Neuronal mechanisms underlying stereopsis: how do simple cells in the visual cortex encode binocular disparity? *Perception* 24: 3–31, 1995.

Ferster D. A comparison of binocular depth mechanisms in areas 17 and 18 of the cat visual cortex. *J Physiol* 311: 623–655, 1981.

Fischer B and Krueger J. Disparity tuning and binocularity of single neurons in cat visual cortex. *Exp Brain Res* 35: 1–8, 1979.

Fischer B and Poggio GF. Depth sensitivity of binocular cortical neurons of behaving monkeys. *Proc R Soc Lond B Biol Sci* 204: 409–414, 1979.

Freeman R and Ohzawa I. On the neurophysiological organisation of binocular vision. *Vision Res* 30: 1661–1676, 1990.

Gardner JC and Raiten EJ. Ocular dominance and disparity-sensitivity: why there are cells in the visual cortex driven unequally by the two eyes. *Exp Brain Res* 64: 505–514, 1986.

Gonzalez F, Perez R, Justo MS, and Ulibarrena C. Binocular interaction and sensitivity to horizontal disparity in visual cortex in the awake monkey. *Int J Neurosci* 107: 147–160, 2001.

LeVay S and Voigt T. Ocular dominance and disparity coding in cat visual cortex. *Vis Neurosci* 1: 395–414, 1988.

Maske R, Yamane S, and Bishop PO. Stereoscopic mechanisms: binocular responses of the striate cells of cats to moving light and dark bars. *Proc R Soc Lond B Biol Sci* 229: 227–256, 1986.

Nieder A and Wagner H. Horizontal-disparity tuning of neurons in the visual forebrain of the behaving barn owl. *J Neurophysiol* 83: 2967–2979, 2000.

Nikara T, Bishop PO, and Pettigrew JD. Analysis of retinal correspondence by studying receptive fields of binocular single units in cat striate cortex. *Exp Brain Res* 6: 353–372, 1968.

Nomura M, Matsumoto G, and Fugiwara S. A binocular model for the simple cell. *Biol Cybern* 63: 237–242, 1990.

Ohzawa I. Mechanisms of stereoscopic vision: the disparity energy model. *Curr Opin Neurobiol* 8: 509–515, 1998.

Ohzawa I, DeAngelis G, and Freeman R. Stereoscopic depth discrimination in the visual cortex: neurons ideally suited as disparity detectors. *Science* 249: 1037–1041, 1990.

Ohzawa I, DeAngelis G, and Freeman R. Encoding of binocular disparity by complex cells in the cat's visual cortex. *J Neurophysiol* 77: 2879–2909, 1997.

Ohzawa I, DeAngelis GC, and Freeman RD. Encoding of binocular disparity by simple cells in the cat's visual cortex. *J Neurophysiol* 75: 1779–1805, 1996.

Ohzawa I and Freeman RD. The binocular organization of complex cells in the cat's visual cortex. *J Neurophysiol* 56: 243–259, 1986a.

Ohzawa I and Freeman RD. The binocular organization of simple cells in the cat's visual cortex. *J Neurophysiol* 56: 221–242, 1986b.

Poggio GF and Fischer B. Binocular interaction and depth sensitivity of striate and prestriate cortex of behaving rhesus monkey. *J Neurophysiol* 40: 1392–1405, 1977.

Poggio GF, Gonzalez F, and Krause F. Stereoscopic mechanisms in monkey visual cortex: binocular correlation and disparity selectivity. *J Neurosci* 8: 4531–4550, 1988.

Poggio GF, Motter BC, Squatrito S, and Trotter Y. Responses of neurons in visual cortex (V1 and V2) of the alert macaque to dynamic random-dot stereograms. *Vision Res* 25: 397–406, 1985.

Poggio GF and Talbot WH. Mechanisms of static and dynamic stereopsis in foveal cortex of the rhesus monkey. *J Physiol* 315: 469–492, 1981.

Prince SJ, Cumming BG, and Parker AJ. Range and mechanism of encoding of horizontal disparity in macaque V1. *J Neurophysiol* 87: 209–221, 2002a.

Prince SJ, Pointon AD, Cumming BG, and Parker AJ. Quantitative analysis of the responses of V1 neurons to horizontal disparity in dynamic random-dot stereograms. *J Neurophysiol* 87: 191–208, 2002b.

Read JCA and Cumming BG. Testing quantitative models of binocular disparity selectivity in primary visual cortex. *J Neurophysiol* 90: 2795–2817, 2003.

Read JCA, Parker AJ, and Cumming BG. A simple model accounts for the reduced response of disparity-tuned V1 neurons to anti-correlated images. *Vis Neurosci* 19: 735–753, 2002.

Smith EL 3rd, Chino YM, Ni J, Ridder WH 3rd, and Crawford ML. Binocular spatial phase tuning characteristics of neurons in the macaque striate cortex. *J Neurophysiol* 78: 351–365, 1997.

Tsao DY, Conway B, and Livingstone MS. Receptive fields of disparity-tuned simple cells in macaque V1. *Neuron* 38: 103–114, 2003.